BIOLOGY OF REPRODUCTION (2012) **87**(2):38, 1–8
Published online before print 23 May 2012.
DOI 10.1095/biolreprod.111.094318

Androgen Initiates Sertoli Cell Tight Junction Formation in the Hypogonadal (*hpg*) Mouse[1]

Mark J. McCabe,[3,4] Charles M. Allan,[5] Caroline F.H. Foo,[3] Peter K. Nicholls,[3,6] Kirsten J. McTavish,[5] and Peter G. Stanton[2,3,6]

[3]*Prince Henry's Institute, Monash Medical Centre, Clayton, Victoria, Australia*
[4]*School of Applied Sciences, Royal Melbourne Institute of Technology University, Bundoora, Victoria, Australia*
[5]*ANZAC Research Institute, University of Sydney, Concord Hospital, Concord, New South Wales, Australia*
[6]*Department of Biochemistry and Molecular Biology, Monash University, Clayton, Victoria, Australia*

ABSTRACT

Sertoli cell tight junctions (TJs) form at puberty as a major component of the blood-testis barrier (BTB), which is essential for spermatogenesis. This study characterized the hormonal induction of functional Sertoli cell TJ formation in vivo using the gonadotropin-deficient hypogonadal (*hpg*) mouse that displays prepubertal spermatogenic arrest. Androgen actions were determined in *hpg* mice treated for 2 or 10 days with dihydrotestosterone (DHT). Follicle-stimulating hormone (FSH) actions were studied in *hpg* mice expressing transgenic human FSH (*hpg*+tgFSH) with or without DHT treatment. TJ formation was examined by mRNA expression and immunolocalization of TJ proteins claudin-3 and claudin-11, and barrier functionality was examined by biotin tracer permeability. Immunolocalization of claudin-3 and claudin-11 was extensive at wild-type (wt) Sertoli cell TJs, which functionally excluded permeability tracer. In contrast, seminiferous tubules of *hpg* testes lacked claudin-3, but claudin-11 protein was present in adluminal regions of Sertoli cells. Biotin tracer permeated throughout these tubules, demonstrating dysfunctional TJs. In *hpg*+tgFSH testes, claudin-3 was generally absent, but claudin-11 had redistributed basally toward the TJs, where function was variable. In *hpg* testes, DHT treatment stimulated the redistribution of claudin-11 protein toward the basal region of Sertoli cells by Day 2, increased *Cldn3* and *Cldn11* mRNA expression, then induced the formation of functional TJs containing both proteins by Day 10. In *hpg*+tgFSH testes, TJ protein redistribution was accelerated and functional TJs formed by Day 2 of DHT treatment. We conclude that androgen stimulates initial Sertoli cell TJ formation and function in mice, whereas FSH activity is insufficient alone, but augments androgen-induced TJ function.

blood-testis barrier, claudin-3, claudin-11, gonadotropins, Sertoli cells, spermatogenesis, tight junctions

INTRODUCTION

The Sertoli cell of the seminiferous epithelium regulates spermatogenesis by providing nutritional and structural support to developing germ cells [1–3]. Early germ cell types (spermatogonia, primary spermatocytes) are located basally to Sertoli cell tight junctions (TJs), which are a major component of the blood-testis barrier (BTB) [4], while meiotic and postmeiotic germ cells (secondary spermatocytes, round and elongate spermatids) are found on the luminal side of the TJs. As the Sertoli cell TJ seals adjacent Sertoli cell membranes, it effectively sequesters adluminal germ cells from the vasculature of the testicular interstitium [5, 6]. Sertoli cell TJs are essential for fertility, and it is well known that their disruption leads to germ cell atresia and cessation of spermatogenesis [6, 7].

Sertoli cell TJs form at puberty in association with an increase in circulating luteinizing hormone (LH)/testosterone and follicle-stimulating hormone (FSH) [7, 8]. Prior to puberty, functional TJs are not present and the epithelium is permeable to tracers including horseradish peroxidase and lanthanum, whereas after puberty, TJs exclude these tracers [9, 10] and contain members of the transmembrane claudin family [11], junctional adhesion molecule (JAM) family [12], and occluding [13] (for reviews see [14, 15]).

Several studies provide direct evidence for the maintenance of TJs by gonadotropins in vitro and in vivo. Testosterone regulates the localization of the two major TJ transmembrane proteins, claudin-11 and occludin, to TJs between immature Sertoli cells in vitro [16, 17], and also stimulates claudin-11 mRNA expression [16, 18]. Consistent with these studies, administration of the androgen-receptor antagonist flutamide to prepubertal and adult rats in vivo disrupted claudin-11 mRNA expression and protein [18]. Alternatively, FSH regulates the localization of claudin-11 to the Sertoli cell TJ in the seasonally regressed testes of the Djungarian hamster in vivo [19]. Recently, we demonstrated the loss of TJ function and TJ protein localization in adult male rats in which circulating gonadotropins were chronically suppressed with the gonadotropin-releasing hormone (GnRH) antagonist acyline [20]. This effect was partially reversible via short-term hormone replacement [20]. Another claudin family member, claudin-3, is found at the Sertoli cell TJ during TJ restructuring as germ cells migrate into the luminal compartment of the seminiferous epithelium in mice and hamsters [21–24] but not rats [16]. In the Sertoli cell-specific androgen-receptor knockout mouse model (SCARKO), claudin-3 mRNA expression was significantly lower than in wild-type (wt) mice, and claudin-3 protein failed to localize to the Sertoli cell TJ [21]. Additionally, a marked decrease in TJ function occurred in the SCARKO

[1]Supported by funds from National Health and Medical Research Council (Australia) Program 494802 (P.G.S) and Project 464857 (C.M.A.) Grants, Australian Research Council Discovery Project DP0881690 (C.M.A.), and by the Victorian Government's Operational Infrastructure Support Program. PHI data audit 10-18.
[2]Correspondence: Peter G. Stanton, Prince Henry's Institute of Medical Research, P.O. Box 5152, Clayton 3168, VIC, Australia.
E-mail: peter.stanton@princehenrys.org

Received: 27 June 2011.
First decision: 26 July 2011.
Accepted: 22 May 2012.

eISSN: 1529-7268 http://www.biolreprod.org
ISSN: 0006-3363

TABLE 1. Primer-specific conditions used for quantitative PCR analysis.

Gene	Species	Accession no.	Primer sequences (5′– 3′)	Size (bp)	[Mg^{2+}] (mM)	Anneal temp. (°C)	Read temp. (°C)*
Cldn11 (Primer3)	Mouse	NM_008770	F: CTACGTGCAGGCTTGTAGAGC R: GGCACATACAGGAAACCAGATG	208	2.5	64	72
Cldn3 (Primer3)	Mouse	NM_009902	F: AACTGCGTACAAGACGAGACG R: GGCACCAACGGGTTATAGAAAT	143	2.5	64	72
Rhox5 [53]	Mouse	NM_008818	F: GCAACACCAGTCCCTGAACA R: CAAAATCTCGGTGTCGCAAA	101	3.5	64	72
Actb [22]	Rat/mouse	NM_031144	F: CCGTAAAGACCTCTATGCCAACA R: GCTAGGAGCCAGGGCAGTAATC	103	2.5	67	72

* Refers to the temperature at which the fluorescence of the PCR product was quantified during LightCycler analysis.

model as shown by permeability to a biotin tracer [21]. Collectively, these data support a role for gonadotropins in the maintenance of functional Sertoli cell TJs in vivo; however, the role of gonadotropins during the initial formation of Sertoli cell TJs in vivo remains unclear.

The aim of this study was to assess hormonal regulation of the initial formation of functional Sertoli cell TJs in vivo through the administration of the potent and nonaromatizable androgen dihydrotestosterone (DHT) to i) the gonadotropin-deficient hypogonadal (*hpg*) mouse and ii) the *hpg*+tgFSH mouse. The *hpg* mouse has a naturally -occurring *Gnrh1* gene deletion, resulting in functional FSH and LH deficiency [25–30]. Spermatogenesis in adult *hpg* testes is arrested at the pachytene stage of meiosis, and TJs appear disorganized by electron microscopy [27, 31–33]. The *hpg*+tgFSH mouse expresses pituitary-independent circulating human FSH [25] at physiological levels that induce incomplete spermatogenic development, which proceeds through meiosis but fails at spermiogenesis [25, 34]. It was hypothesized that Sertoli cell TJs are structurally impaired and nonfunctional in *hpg* and *hpg*+tgFSH mice, providing a valuable experimental platform to investigate the role of androgen (via DHT), with or without FSH activity, during the initial formation of functional Sertoli cell TJs in vivo.

MATERIALS AND METHODS

Animals

Male gonadotropin-deficient *hpg* and *hpg*+tgFSH mice (αβ.6 line, expressing human FSH under a pituitary-independent rat insulin promoter II) were previously described [25, 33]. All animal work was approved by the South West Area Health Services Animal Ethics Committee. Operative procedures were conducted under 0.5% ketamine (Parke-Davis, Caringbah, NSW, Australia) and xylazine (0.01 ml/g body weight; Bayer Australia Ltd., Botany, NSW, Australia) anesthesia, which was administered by an i.p. injection [35]. At the end of experimentation, mice were killed by anesthetic overdose.

Experimental Design

DHT (Merck, Darmstadt, Germany) was administered to adult (3–4 mo old) *hpg* and *hpg*+tgFSH mice via a 1-cm SILASTIC (Dow Corning, Midland, MA) implant placed subdermally for 2 or 10 days (n = 3 per group) [33]. DHT-treated mice and age-matched, untreated wt, *hpg*, and *hpg*+tgFSH males (n = 3–5 per group) were killed on the same day. Testes were excized, trimmed, and weighed, and a slit was cut into the tunica albuginea of the left testis, after which it was incubated in NHS-linked biotin (10 mg/ml in PBS/0.01 M $CaCl_2$; EZ-Link Sulfo-NHS-LC-Biotin; Pierce, Rockford, IL) for 30 min at room temperature [20, 22]. This technique is a minor modification to that used previously [20, 22], as the small size of the *hpg* testes (~2 mg) meant that administration of tracer by intratesticular injection was not possible. Therefore, we compared biotin permeation into adult wt mouse testes by i) intratesticular injection and ii) immersion of the testes in biotin solution with or iii) without a small slit in the tunica albuginea [21]. No differences in biotin permeation were observed between these methods (data not shown), and we chose the method described above. Testes were then immersion fixed in Bouin solution (4 h) and stored in 70% ethanol for immunohistochemical analysis. The right testis from each mouse was immediately snap frozen in liquid nitrogen for RT-PCR analysis.

Immunohistochemistry

Tissues were embedded in paraffin wax, and 5-μm sections were mounted onto Superfrost-Plus slides (HD Scientific, Melbourne, VIC, Australia) and dried overnight at 37°C. For morphological analysis, sections were stained with hematoxylin and eosin, and measurements of tubule diameter and lumen diameter were collected from n = 3 animals per group, with n = 3 different sections per animal and n = 10 measurements within each section. Measurements were recorded using AnalySIS software (Olympus Australia, Mt. Waverley, VIC, Australia), and the mean and standard deviation for each group were determined. For immunohistochemical analysis, antigen retrieval was performed by heating the sections for 10 min in 600 ml of 1 mM Ethylenediaminetetraacetic acid-NaOH (pH 8.0) [36] in an 800 W microwave. Sections were then allowed to cool (1 h) before washing for 5 min in MilliQ water (Millipore, Billerica, MA) and blocked in 10% (v/v) normal goat serum and 10% (v/v) CAS Block (Invitrogen, Carlsbad, CA) for 1 h. Primary antibodies, rabbit anti-claudin-11 (1.25 μg/ml, overnight; #36-4500; Zymed, San Francisco, CA), rabbit anti-claudin-3 (1.25 μg/ml, overnight; #36-1700; Zymed), and mouse anti-connexin-43 (1:400, overnight; #C8093; Sigma) were diluted in 10% normal goat serum (Chemicon International, Temecula, CA) in PBS and applied to the sections at 25°C. Negative controls substituted rabbit IgG at the same concentration for the primary antibody. Sections were then washed in PBS before incubation (30 min) with goat anti-rabbit/mouse Alexa-488/546 (Molecular Probes, Eugene, OR) at a 1:400 dilution, and were then mounted with FluorSave (Calbiochem, La Jolla, CA) and visualized by confocal microscopy (Fluoview FV300; Olympus).

For qualitative TJ functional analysis, the biotin tracer was visualized directly using streptavidin Alexa-488 (Molecular Probes) diluted 1:100 in the secondary antibody solution. Negative controls for biotin staining omitted the streptavidin Alexa-488 reagent.

Total RNA Extraction and Quantitative Real-Time RT-PCR Analyses

Total RNA was extracted from frozen mice testes using the RNA Isolation Kit (Qiagen, Hildens, Germany), and contaminating DNA was removed from the extract by a DNA-free kit (Ambion; Life Technologies, Carlsbad, CA) according to the manufacturer's instructions. Reverse-transcription used AMV-Reverse Transcriptase (Roche, Mannheim, Germany) and random hexamers as described elsewhere [16].

Expression of mRNA was quantified using the Roche Light Cycler (Roche) and FastStart DNA Master Sybr Green 1 systems (Roche). Oligonucleotide primer pair sequences for the Sertoli cell genes *Cldn11*, *Cldn3*, and *Rhox5* were obtained from published sources or were designed using the Primer3 program online and ordered from Sigma Genosys (Castle Hill, NSW, Australia). Primer details and PCR conditions, including anneal temperature, elongation time, and Mg^{2+} concentration, are presented in Table 1. Primers produced a single band on DNA agarose gels that corresponded to the target protein as shown by DNA sequencing (data not shown). Standard curves for PCR analyses were generated using dilutions of an adult wt mouse testicular cDNA preparation of arbitrary units. Unless otherwise noted, PCR of all samples was performed using duplicate reactions for 38 cycles, after which a melting curve analysis was performed to monitor PCR product purity (see Table 1). Expression data for Sertoli cell-specific transcripts (*Cldn3, Cldn11, Rhox5*) were first normalized to the housekeeper gene, *Actb*, and then adjusted by a two-step procedure recently

described [37] to correct for the differences in total Sertoli cell number between the *hpg*, *hpg*+TgFSH, and wt testes (1.29 million, 2.32 million, and 5.15 million cells per testis, respectively [34]). The dilution effect in total testicular RNA caused by increased RNA from proliferating germ cells was then corrected for based on ratios of testis weights as described in detail elsewhere [36]. DHT has no effect on Sertoli cell number in *hpg* testes [33].

Statistical Analysis

Statistical analysis was performed using SigmaStat for Windows (version 3.5; Jandel Corporation, San Rafael, CA). Treatments were compared to controls by ANOVA followed by the Student Newman-Keuls test, or where data was nonparametric, Kruskal-Wallis test, followed by Newman-Keuls analog (equal *N*s). $P < 0.05$ was used to determine if results were statistically significant, and data has been expressed as the mean ± SD, with n = 3–5 mice per group.

RESULTS

Testis Weights ± DHT Treatment

Untreated *hpg* testis weights were at 2.5% ($P < 0.001$) of wt testis weights, similar to published data [33], while the untreated *hpg*+tgFSH testis weights were at 17.0% ($P < 0.001$) of wt testis weights and 7-fold larger ($P < 0.001$) than the untreated *hpg* testis weights (Fig. 1A).

No significant change in testis weights was observed in DHT-treated *hpg* mice until 10 days of treatment, when the testes had increased to 7.8% ($P = 0.016$) of wt values (Fig. 1A). DHT treatment of *hpg*+tgFSH mice did not significantly alter testis weights after 2 or 10 days of treatment compared to untreated controls (Fig. 1A), which is likely to reflect variable testis weights in the untreated *hpg*+tgFSH mice used in this study.

Development of TJ Functionality and TJ Protein Localization in hpg *and* hpg+*tgFSH Testes ± DHT Treatment*

Tubule lumen presence and/or formation is a surrogate measure of TJ functionality [38, 39]. Tubules of untreated *hpg* testes, or *hpg* animals treated with DHT for 2 days, did not generally contain lumens as shown morphologically (Fig. 1B) or following quantification of lumen diameter (Fig. 2A); however, a small percentage (<3%) of the total tubules examined did show some lumen formation (Fig. 2C). After 10 days of DHT stimulation in *hpg* animals, lumens were clearly present (Fig. 1B) in all tubules (Fig. 2C), although these were smaller than wt animals (Fig. 2A). Lumens were identified in 25% of *hpg*+tgFSH tubules (Fig. 2C), but in contrast to the *hpg* testis, lumen formation had occurred in all tubules after 2 days of DHT treatment in *hpg*+tgFSH mice (Figs. 1B and 2, A and C). Changes in tubule diameter occurred in parallel with lumen diameter following 10 days of DHT treatment of *hpg* mice, but no effect of the androgen on tubule diameter was observed in the *hpg*+tgFSH groups (Fig. 2B). It is noted that postmeiotic elongating spermatids were present in some tubules from both the *hpg* and *hpg*+tgFSH groups treated with DHT for 10 days (Fig. 1B).

We then assessed TJ functionality using the biotin tracer permeability method. Biotin staining was extensive in the interstitium of wt testes and only entered the seminiferous tubules as far as the inter-Sertoli cell TJ, as shown by marked immunostaining for claudin-11 and claudin-3 (Fig. 3, A and B). In the *hpg* testis, biotin staining was present in the interstitium and also permeated around all cells within the seminiferous epithelium (Fig. 3). Claudin-11 staining remained present but was no longer located basally; instead, staining was predominant in adluminal regions of Sertoli cells (Fig. 3A). Claudin-3 staining was essentially undetectable in the seminiferous

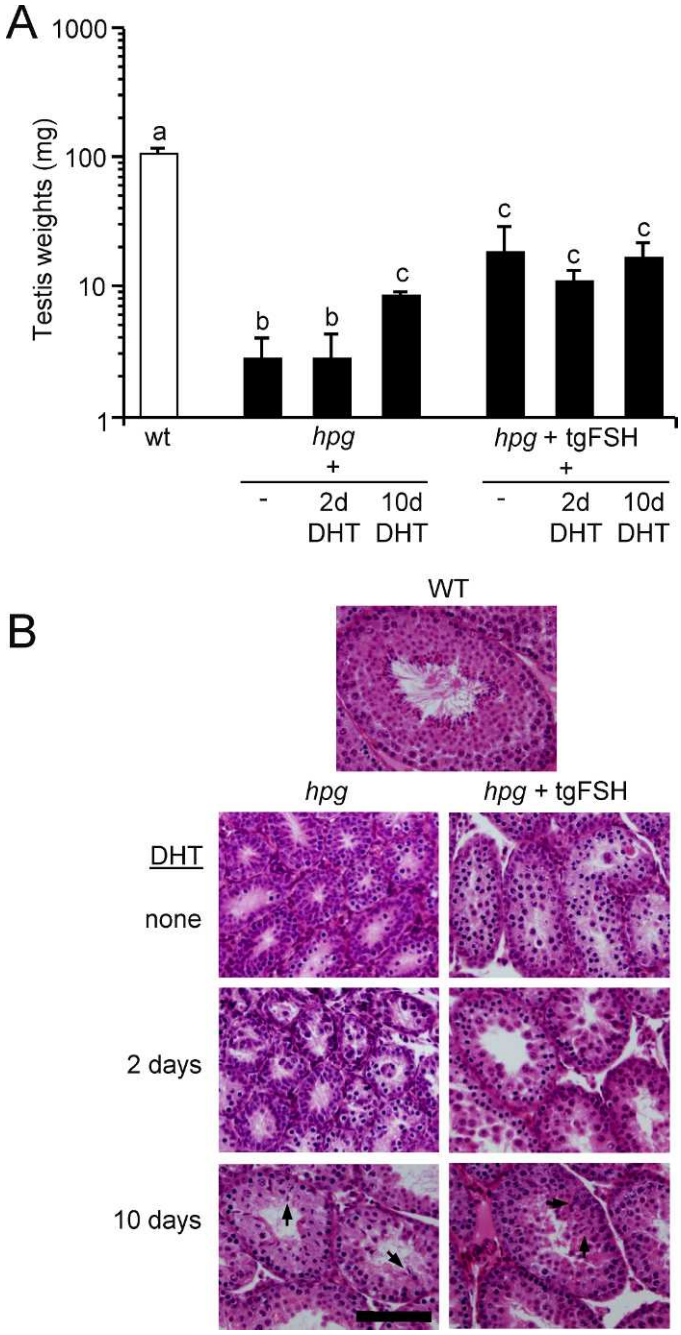

FIG. 1. Changes in testis weights (**A**) and lumen formation (**B**), following DHT treatment. **A**) Testes from wt, *hpg*, and *hpg*+tgFSH mice treated with DHT for 2 and 10 days were dissected from the mice and trimmed of all fat, epididymides, and connective tissue immediately after death and weighed prior to further treatment. Data is mean ± SD, n = 3 per group. a versus b/c, $P < 0.001$; b versus c, $P < 0.01$. Note the log scale on the y-axis. **B**) Testicular histology for the same groups as **A**. Sections (5 μm) are stained with hemotoxylin and eosin. Arrows indicate the presence of postmeiotic elongating spermatids in the 10-day DHT treatment groups. Bar = 50 μm.

epithelium of *hpg* testes, with apparent interstitial staining also detected in the negative control (see insert in wt panel, Fig. 3B). After 2 days of DHT treatment to *hpg* mice, seminiferous tubules remained permeable to the biotin tracer, which was present both in the interstitium and epithelium, whereas claudin-11 staining remained adluminal but had redistributed basally compared with staining in untreated *hpg* testes (Fig.

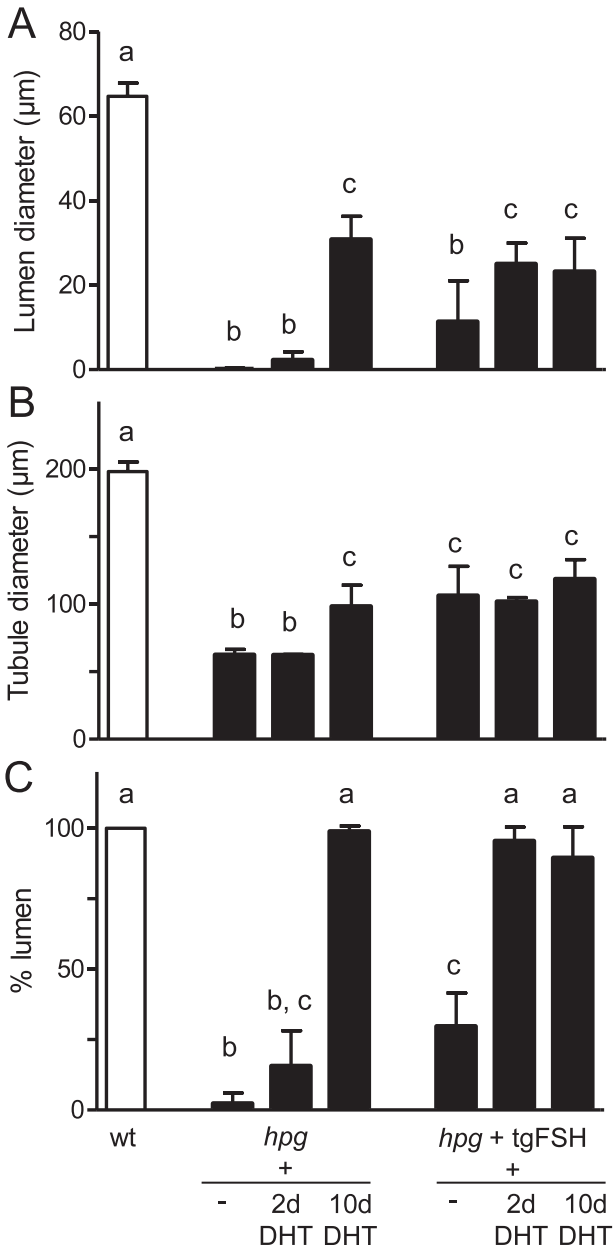

FIG. 2. Changes in lumen diameter (**A**), tubule diameter (**B**), and percentage of tubules that contained a lumen (**C**) following DHT treatment. Lumen diameters (μm; **A**) and tubule diameters (μm; **B**) were quantified in testes from wt, *hpg*, and *hpg*+tgFSH mice treated with DHT for 2 and 10 days. The percentage of tubules that contained a lumen in the same treatment group is shown in **C**. Data is mean ± SD, n = 3 per group. Different letters indicate significant differences between groups ($P < 0.05$ or greater).

3A). Claudin-3 staining was still not detectable in the epithelium at 2 days of DHT administration (Fig. 3B). After 10 days of DHT treatment, biotin staining was excluded from most tubules and remained in the interstitium of *hpg* testes, similar to the phenotype of the wt testes (Fig. 3). Claudin-11 staining was now predominantly found at basally located inter-Sertoli cell TJs, which also contained detectable claudin-3 (Fig. 3B).

In *hpg*+tgFSH testes, biotin staining was present in the interstitium and permeated throughout some of the seminiferous tubules but was excluded from others (Fig. 3, A and B), although few tubules contained distinct lumens (Figs. 1B and 2C). Claudin-11 staining was present but disorganized in the basal area of Sertoli cells just adluminal to the basement membrane, while claudin-3 was generally absent, although minor staining for basally located claudin-3 in some tubules was observed (data not shown).

After 2 or 10 days of DHT treatment, biotin staining was excluded from most of the seminiferous tubules of *hpg*+tgFSH testes and permeated only as far as claudin-11 staining, which was extensive at basally located TJs (Fig. 3A). As also observed in the *hpg* model, redistribution of adluminal claudin-11 protein occurred in an apical-to-basal manner, evident by comparison of staining patterns at 2 and 10 days of DHT treatment. Claudin-3 staining was more prominent at the TJ at both these time points than in the *hpg* mouse, but staining was not extensive (Fig. 3B).

Effect of DHT Treatment on Testicular Gap Junction Protein Localization

Recent data suggests that gap junctions, which are also present at the BTB, can regulate BTB dynamics via negative regulation of TJ proteins and the intracellular adaptor protein, ZO-1, which is common to both tight and gap junctions [40]. Therefore, we examined the regulation of gap junctions in the *hpg* model by colocalization of connexin-43 with claudin-11 (Fig. 3C). In wt mice, connexin-43 and claudin-11 were colocalized at basally located Sertoli cell junctions. In *hpg* mice, connexin-43 no longer colocalized with claudin-11, but staining for both proteins was similar as it was predominantly localized adluminally (Fig. 3C). DHT treatment of *hpg* mice restored colocalization of both connexin-43 and claudin-11 at basally located Sertoli cell junctions, but this took 10 days to occur, mirroring the time course of restoration of BTB function as shown by biotin tracer permeation (Fig. 3A).

Interestingly, there appeared to be less connexin-43 staining in the *hpg*+tgFSH testis compared with the *hpg* model (Fig. 3C), and most staining was at basally located junctions. DHT treatment for 2 days caused a rapid re-appearance of connexin-43 in an adluminal location (Fig. 3C), and this staining was redistributed to basal junctions following 10 days of DHT treatment, in a manner similar to that of claudin-11.

Effects of DHT Treatment on mRNA Expression in hpg *and* hpg+*tgFSH Mice*

To confirm the induction of androgen actions by the DHT implants, the expression of an androgen-regulated Sertoli cell gene, *Rhox5* [41], was determined by qPCR. Relative *Rhox5* mRNA expression was 100-fold ($P < 0.001$) less in *hpg* compared to that in wt testes, but was increased 42-fold ($P < 0.001$) by 2 days of DHT treatment and remained at high levels at 10 days of DHT treatment (Fig. 4A). In contrast, *Rhox5*

FIG. 3. Assessment of TJ functionality and TJ protein localization following DHT treatment of *hpg* and *hpg*+tgFSH mice. *hpg* and *hpg*+tgFSH mice were treated with DHT for 2 and 10 days before assessment of TJ permeability with a biotin tracer (green) and TJ protein localization with claudin-11 (**A**, red) and claudin-3 (**B**, red). * indicates adluminal staining of claudin-11. **C**) Localization of claudin-11 (green) with the gap junction protein connexin-43 (red). Bar = 50 μm. Insets = negative controls.

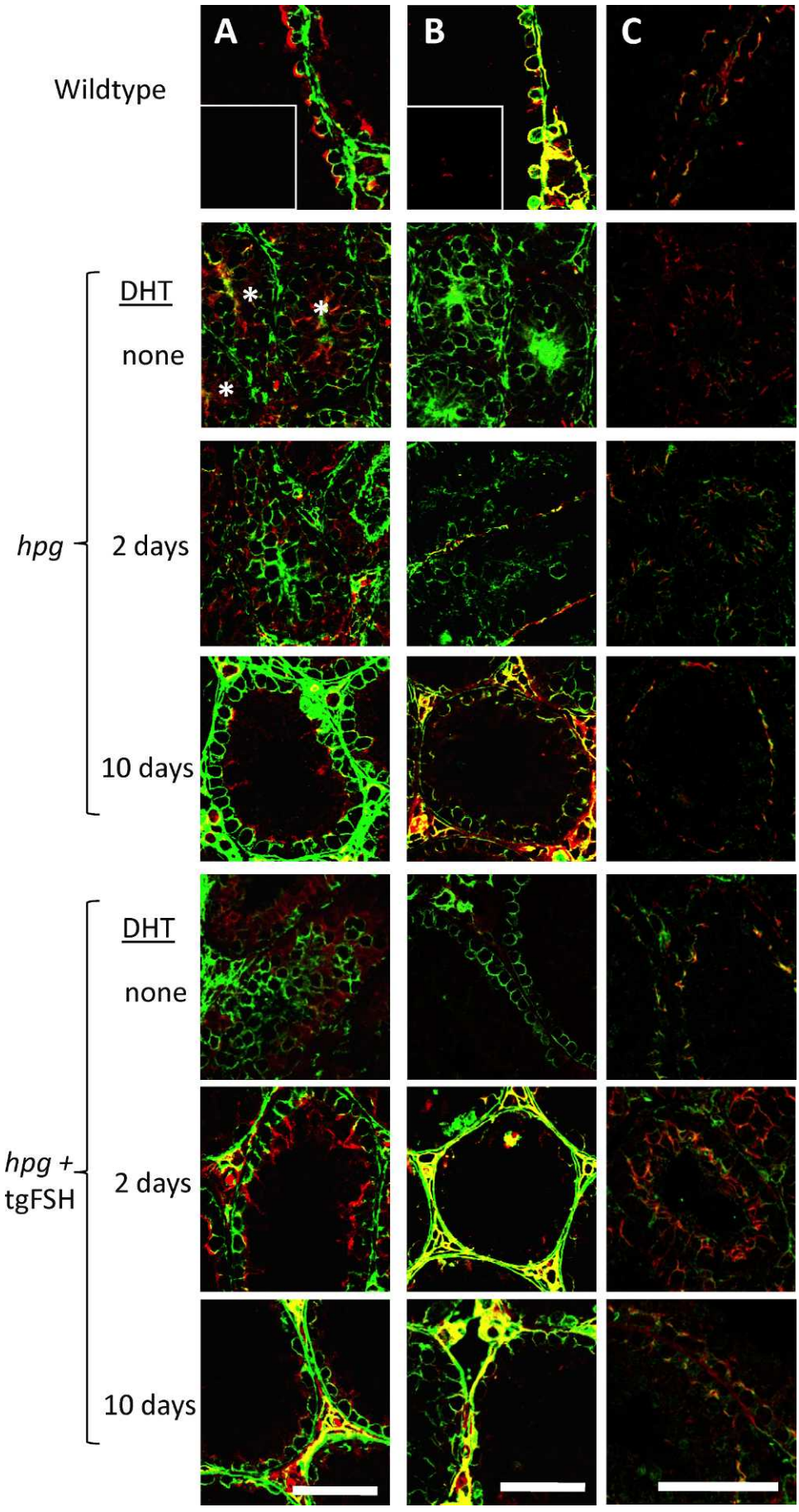

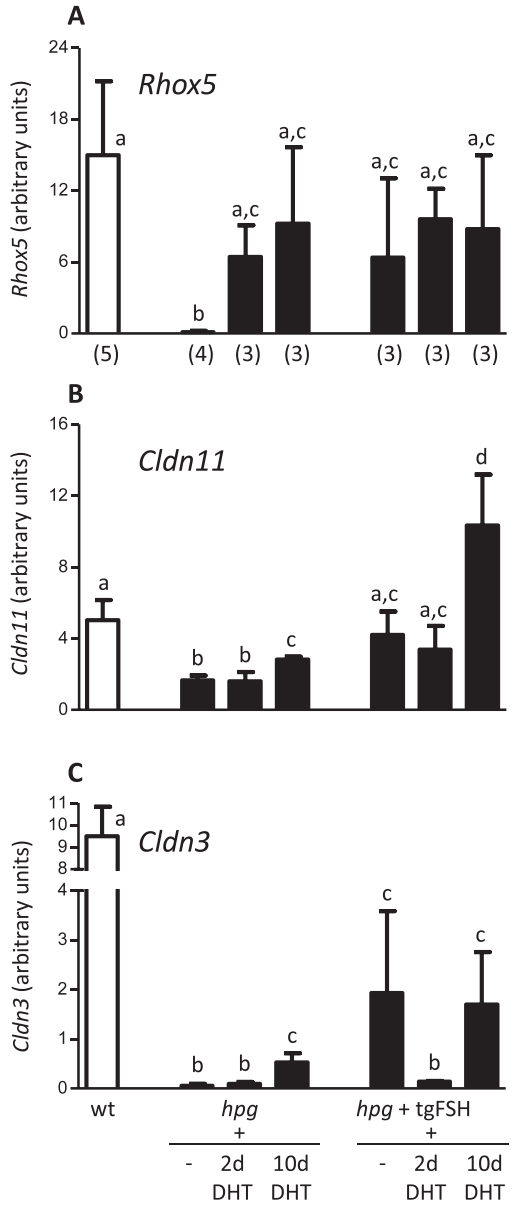

FIG. 4. Total testis *Rhox5*, *Cldn-11*, and *Cldn-3* expression levels in response to DHT treatment in *hpg* and *hpg*+tgFSH mice. Total RNA was extracted from frozen testes and reverse transcribed for real-time quantitative PCR analysis of the Sertoli cell androgen-regulated gene *Rhox5* (**A**), *Cldn11* (**B**), and *Cldn3* (**C**) in adult wt mice, adult *hpg*, and *hpg*+tgFSH mice that had received the pure androgen DHT for 2 days and 10 days. The measured mRNA transcripts were adjusted for *Actb* (housekeeping gene as loading control), plus differences in Sertoli cell number and testis weight (to account for dilution by germ cells) as detailed in the text. Data is mean ± SD, n = 3–5 per group (as indicated in **A**). Different letters indicate significant differences between groups with $P < 0.05$ or as specified in the text.

mRNA expression in the *hpg*+tgFSH mouse was not significantly different than that in the wt mouse (Fig. 4A), and DHT treatment did not significantly alter *Rhox5* expression in this model (Fig. 4A).

Relative expression levels of Sertoli cell *Cldn11* mRNA were 3-fold ($P < 0.001$) less in *hpg* compared to those in wt mice and were significantly increased ($P = 0.011$) in the 10 day DHT treatment group (Fig. 4B). Administration of DHT to *hpg*+tgFSH mice for 10 days also increased *Cldn11* expression levels 3-fold ($P = 0.001$; Fig. 4B). Relative *Cldn3* levels in *hpg* testes were >100-fold less than those in wt testes ($P < 0.001$) and were upregulated 8-fold ($P = 0.001$) by 10 days of DHT treatment (Fig. 4C). In contrast, *Cldn3* expression levels in the *hpg*+tgFSH were only 8-fold less than those in the wt ($P < 0.001$), and no trend was observable with DHT treatment, although significant within-group animal variation in the untreated mice may have masked any androgen effects.

DISCUSSION

Androgen and FSH have established roles regulating Sertoli cell TJ function in mature testes; however, there has been little direct investigation of hormonal requirements for the initial formation of TJs in vivo. This study used a naturally occurring model of gonadotropin deficiency, the *hpg* mouse, to investigate TJ formation in vivo during the selective hormonal maturation of prepubertal testes. We showed that the hormone-deficient background of the *hpg* testes results in the absence of normal Sertoli cell TJ assembly and function. The present findings reveal that androgen actions alone stimulate the development of structurally and functionally competent Sertoli cell TJs in *hpg* testes. FSH actions alone were insufficient to induce the completion of Sertoli cell TJ formation in the *hpg*+tgFSH model; however, FSH activity markedly enhanced androgen-induction of functional Sertoli cell TJs.

Androgen induction of Sertoli cell TJ formation was determined by administration of DHT at a dose that provides maximal androgen-specific initiation of qualitatively normal spermatogenic development in *hpg* testes [33]. Males were treated with DHT rather than testosterone to avoid aromatization of administered androgen to estradiol, which can induce pituitary FSH secretion in *hpg* mice [31, 37, 42]. As such, endogenous serum FSH levels in DHT-treated *hpg* mice remained at less than 4% of wt values, similar to untreated *hpg* mice [30], meaning that the effects seen for DHT in these animals were independent of significant FSH activity. In this study, short-term DHT treatment for 10 days increased *hpg* testis weights and seminiferous tubule diameters to a similar extent as described elsewhere [42], and also increased the expression of *Rhox5*, a known androgen-dependent and Sertoli cell-specific gene in the postnatal testis [41, 43].

The ability of FSH to stimulate Sertoli cell TJ formation was determined using *hpg*+tgFSH mice [25], in which pituitary-independent FSH expression allowed investigation of FSH action in isolation or combined with DHT [34]. Interestingly, testis weights in *hpg*+tgFSH mice treated with DHT were not significantly increased by 10 days, which we ascribed to larger than expected, untreated *hpg*+tgFSH testes in this study. Likewise, *Rhox5* expression was not significantly increased in DHT-treated compared to untreated *hpg*+tgFSH testes, due to individual variations within the untreated *hpg*+tgFSH group. However, elevated Sertoli cell *Rhox5* expression in untreated *hpg*+tgFSH compared to non-tg *hpg* testes supports recent work describing increased testicular *Rhox5* expression after treatment of *hpg* males with exogenous FSH [44], thus providing strong in vivo evidence for FSH-regulated *Rhox5* transcription. Postmeiotic spermatids were consistently observed in DHT-treated *hpg* and *hpg*+tgFSH testes after 10 days, which, when combined with changes in mRNA expression and localization of TJ proteins in these testes (see below), all demonstrate androgen-initiated spermatogenic development. Although not quantitated in this study, it is expected that DHT-stimulated spermatid numbers would be greater in the *hpg*+tgFSH testis rather than the *hpg* testis, based on the known ability of FSH to stimulate additional round spermatid formation in androgen-treated *hpg* mice [34, 42].

Additionally, while factors locally secreted by meiotic and postmeiotic germ cells may contribute to TJ protein localization and BTB function (e.g., TGFβ3 [17], GDF9 [45], for review see [46]), the available data suggests a negative impact of these factors on BTB function, with no positive mediators yet described.

Our data show differential regulation of the two TJ proteins claudin-11 and claudin-3 in the *hpg* testis, which we have demonstrated, by biotin tracer permeability, has a nonfunctional BTB. Claudin-11 protein was present, but in a disorganized pattern in adluminal regions of Sertoli cells at the center of the tubules, whereas claudin-3 protein was undetectable. In adult wt mice, both proteins are found in functional Sertoli cell TJs, but claudin-3 is only transiently expressed during stages VII–X when premeiotic germ cells translocate across the BTB [21, 23, 24], whereas claudin-11 is present across all stages. Hence, it is currently believed that claudin-3 is involved in newly formed TJs that appear during BTB remodeling [23], and its absence in the *hpg* testis is consistent with the lack of functionality of the BTB. Additionally, the disorganized claudin-11 pattern and lack of claudin-3 in *hpg* mice are consistent with other observations that inter-Sertoli cell junctional complexes, which include TJs and gap junctions [7], are rudimentary in this model [32]. In other animal models where circulating levels of gonadotropins are reduced, either by GnRH antagonist treatment [20] or by a change in photoperiod [19, 22], we have also demonstrated that key Sertoli cell TJ proteins such as claudin-11 or occludin remain present in the epithelium, albeit localized away from the TJ in the center of the seminiferous tubules.

Androgen action for 2 days failed to elevate *Cldn11* or *Cldn3* mRNA levels in *hpg* testes but initiated the redistribution of existing claudin-11 protein basally; however, TJs remained dysfunctional in *hpg* mice, and lumen formation was rare at this time point. Additionally, no claudin-3 protein was detectable. These observations support in vitro data indicating that androgen promotes the endocytic recycling of internalized TJ proteins back to the Sertoli cell surface [16, 17, 47]. Thus, our findings are consistent with endosomal recycling of claudin-11 as an androgen-dependent mechanism, which may be initiated before transcription of TJ proteins in the *hpg* mouse in vivo. After 10 days of DHT treatment of the *hpg* animal, both claudin-11 and claudin-3 mRNA expression were upregulated, and both proteins were extensively immunolocalized at functional TJs. These data are consistent with the known androgen dependency of claudin-3 in the mouse [21] and the involvement of claudin-3 in newly formed TJs [23].

In comparison to the *hpg* model, TJ protein localization and function were, in general, promoted by FSH action in the *hpg*+tgFSH testis. In untreated animals, TJ barrier functionality varied from functional to dysfunctional between tubules, indicating that the action of FSH may partially initiate the formation of TJs in this model. In view of the potential for synergistic FSH and androgen activity in the development of *hpg* testes [34, 42], it is also possible that basal concentrations of intratesticular testosterone in *hpg*+tgFSH mice (at levels equal to those of non-tg *hpg* or 15%–17% of those of wt [34]) may also contribute to some degree of Sertoli cell TJ development, which is consistent with previous reports of sparsely distributed postmeiotic elongated spermatids in tubules from *hpg*+tgFSH testes [25, 34].

In *hpg*+tgFSH testes, claudin-11 immunostaining appeared marginally adluminal to the TJ, and claudin-3 staining was occasionally detected. More intense claudin-3 staining at the TJ was observed after just 2 days of DHT treatment, despite no increase in relative testicular *Cldn3* mRNA expression. This more rapid appearance of claudin-3 protein may indicate that FSH directly stimulates testicular claudin-3 protein relocalization, as we recently observed in the hamster [22], which is consistent with the priming role that FSH exerts in the regulation of Sertoli cell-germ cell adhesion junctions [48–51]. This relocalization of claudin-3 could include a component of endocytic recycling, as observed for claudin-11 in the *hpg* animal [16, 17, 47]. Hence, we propose that a key role of gonadotropins (FSH- and LH-stimulated androgen activity) is to promote the synthesis and redistribution of Sertoli cell TJ proteins to the BTB in vivo.

Recent analysis of TJ and gap junction marker proteins in the connexin-43 knockout mouse has suggested that Sertoli cell connexin-43 channels may mediate BTB function [40, 52]. In both the *hpg* and *hpg*+tgFSH models reported here, connexin-43 protein localization was essentially similar to claudin-11, with both proteins present at basally located junctions when the BTB was functional, or adluminally located in Sertoli cells when the BTB was non-functional. Although this data supports a role for gonadotropin regulation of testicular gap junctions, it does not allow any further dissection of the interplay between TJs and gap junctions at the BTB.

In summary, we have used DHT-induced *hpg* testis development to determine the contribution of androgen and FSH in Sertoli cell TJ formation. It is proposed that gonadotropins (via FSH- and LH-stimulated androgen activity) regulate the postnatal formation of a functionally competent Sertoli cell TJ in the mouse by a temporal mechanism, which includes the redistribution of existing claudin-11 protein and the appearance of claudin-3 protein to/at the Sertoli cell TJ, combined with stimulation of *Cldn3* and *Cldn11* mRNA expression. Androgen actions alone stimulated the initial expression and localization of these TJ proteins at basally located and functional Sertoli cell TJs. It is further concluded that while FSH alone stimulated partial TJ formation in the mouse, its actions markedly enhanced the androgen induction of complete TJ formation and function.

ACKNOWLEDGMENT

The authors acknowledge Mathew Robson and Mark Jimenez for expert technical assistance and Professor David Handelsman for access to the *hpg* mouse model.

REFERENCES

1. Aravindan GR, Mruk D, Lee WM, Cheng CY. Identification, isolation, and characterization of a 41-kilodalton protein from rat germ cell-conditioned medium exhibiting concentration-dependent dual biological activities. Endocrinology 1997; 138:3259–3268.
2. Cheng CY, Mruk DD. Cell junction dynamics in the testis: Sertoli-germ cell interactions and male contraceptive development. Physiol Rev 2002; 82:825–874.
3. Griswold MD. The central role of Sertoli cells in spermatogenesis. Semin Cell Dev Biol 1998; 9:411–416.
4. Setchell BP. Hormones: what the testis really sees. Reprod Fertil Dev 2004; 16:535–545.
5. Chung NP, Cheng CY. Is cadmium chloride-induced inter-sertoli tight junction permeability barrier disruption a suitable in vitro model to study the events of junction disassembly during spermatogenesis in the rat testis? Endocrinology 2001; 142:1878–1888.
6. Chung NP, Mruk D, Mo MY, Lee WM, Cheng CYA. 22-amino acid synthetic peptide corresponding to the second extracellular loop of rat occludin perturbs the blood-testis barrier and disrupts spermatogenesis reversibly in vivo. Biol Reprod 2001; 65:1340–1351.
7. Russell LD, Peterson RN. Sertoli cell junctions: morphological and functional correlates. Int Rev Cytol 1985; 94:177–211.
8. Vitale R, Fawcett DW, Dym M. The normal development of the blood-testis barrier and the effects of clomiphene and estrogen treatment. Anat Rec 1973; 176:331–344.

9. Pelletier RM. Cyclic formation and decay of the blood-testis barrier in the mink (*Mustela vison*), a seasonal breeder. Am J Anat 1986; 175:91–117.
10. Pelletier RM. Cyclic modulation of Sertoli cell junctional complexes in a seasonal breeder: the mink (*Mustela vison*). Am J Anat 1988; 183:68–102.
11. Morita K, Sasaki H, Fujimoto K, Furuse M, Tsukita S. Claudin-11/OSP-based tight junctions of myelin sheaths in brain and Sertoli cells in testis. J Cell Biol 1999; 145:579–588.
12. Gliki G, Ebnet K, Aurrand-Lions M, Imhof BA, Adams RH. Spermatid differentiation requires the assembly of a cell polarity complex downstream of junctional adhesion molecule-C. Nature 2004; 431: 320–324.
13. Saitou M, Furuse M, Sasaki H, Schulzke JD, Fromm M, Takano H, Noda T, Tsukita S. Complex phenotype of mice lacking occludin, a component of tight junction strands. Mol Biol Cell 2000; 11:4131–4142.
14. Wong CH, Cheng CY. The blood-testis barrier: its biology, regulation, and physiological role in spermatogenesis. Curr Top Dev Biol 2005; 71: 263–296.
15. Pelletier RM. The blood-testis barrier: the junctional permeability, the proteins and the lipids. Prog Histochem Cytochem 2011; 46:49–127.
16. Kaitu'u-Lino TJ, Sluka P, Foo CF, Stanton PG. Claudin-11 expression and localisation is regulated by androgens in rat Sertoli cells in vitro. Reproduction 2007; 133:1169–1179.
17. Su L, Mruk DD, Lee WM, Cheng CY. Differential effects of testosterone and TGF-beta3 on endocytic vesicle-mediated protein trafficking events at the blood-testis barrier. Exp Cell Res 2010; 316:2945–2960.
18. Florin A, Maire M, Bozec A, Hellani A, Chater S, Bars R, Chuzel F, Benahmed M. Androgens and postmeiotic germ cells regulate claudin-11 expression in rat Sertoli cells. Endocrinology 2005; 146:1532–1540.
19. Tarulli GA, Stanton PG, Lerchl A, Meachem SJ. Adult sertoli cells are not terminally differentiated in the Djungarian hamster: effect of FSH on proliferation and junction protein organization. Biol Reprod 2006; 74: 798–806.
20. McCabe MJ, Tarulli GA, Meachem SJ, Robertson DM, Smooker PM, Stanton PG. Gonadotropins regulate rat testicular tight junctions in vivo. Endocrinology 2010; 151:2911–2922.
21. Meng J, Holdcraft RW, Shima JE, Griswold MD, Braun RE. Androgens regulate the permeability of the blood-testis barrier. Proc Natl Acad Sci U S A 2005; 102:16696–16700.
22. Tarulli GA, Meachem SJ, Schlatt S, Stanton PG. Regulation of testicular tight junctions by gonadotrophins in the adult Djungarian hamster in vivo. Reproduction 2008; 135:867–877.
23. Komljenovic D, Sandhoff R, Teigler A, Heid H, Just WW, Gorgas K. Disruption of blood-testis barrier dynamics in ether-lipid-deficient mice. Cell Tissue Res 2009; 337:281–299.
24. Chihara M, Otsuka S, Ichii O, Hashimoto Y, Kon Y. Molecular dynamics of the blood-testis barrier components during murine spermatogenesis. Mol Reprod Dev 2010; 77:630–639.
25. Allan CM, Haywood M, Swaraj S, Spaliviero J, Koch A, Jimenez M, Poutanen M, Levallet J, Huhtaniemi I, Illingworth P, Handelsman DJ. A novel transgenic model to characterize the specific effects of follicle-stimulating hormone on gonadal physiology in the absence of luteinizing hormone actions. Endocrinology 2001; 142:2213–2220.
26. Cattanach BM, Iddon CA, Charlton HM, Chiappa SA, Fink G. Gonadotrophin-releasing hormone deficiency in a mutant mouse with hypogonadism. Nature 1977; 269:338–340.
27. Charlton HM, Halpin DM, Iddon C, Rosie R, Levy G, McDowell IF, Megson A, Morris JF, Bramwell A, Speight A, Ward BJ, Broadhead J, et al. The effects of daily administration of single and multiple injections of gonadotropin-releasing hormone on pituitary and gonadal function in the hypogonadal (hpg) mouse. Endocrinology 1983; 113:535–544.
28. Huang HF, Marshall GR, Rosenberg R, Nieschlag E. Restoration of spermatogenesis by high levels of testosterone in hypophysectomized rats after long-term regression. Acta Endocrinol (Copenh) 1987; 116:433–444.
29. Mason AJ, Hayflick JS, Zoeller RT, Young WS III, Phillips HS, Nikolics K, Seeburg PH. A deletion truncating the gonadotropin-releasing hormone gene is responsible for hypogonadism in the hpg mouse. Science 1986; 234:1366–1371.
30. Jimenez M, Spaliviero JA, Grootenhuis AJ, Verhagen J, Allan CM, Handelsman DJ. Validation of an ultrasensitive and specific immunofluorometric assay for mouse follicle-stimulating hormone. Biol Reprod 2005; 72:78–85.
31. Ebling FJ, Brooks AN, Cronin AS, Ford H, Kerr JB. Estrogenic induction of spermatogenesis in the hypogonadal mouse. Endocrinology 2000; 141: 2861–2869.
32. Myers M, Ebling FJ, Nwagwu M, Boulton R, Wadhwa K, Stewart J, Kerr JB. Atypical development of Sertoli cells and impairment of spermatogenesis in the hypogonadal (hpg) mouse. J Anat 2005; 207:797–811.
33. Singh J, O'Neill C, Handelsman DJ. Induction of spermatogenesis by androgens in gonadotropin-deficient (hpg) mice. Endocrinology 1995; 136:5311–5321.
34. Haywood M, Spaliviero J, Jimemez M, King NJ, Handelsman DJ, Allan CM. Sertoli and germ cell development in hypogonadal (hpg) mice expressing transgenic follicle-stimulating hormone alone or in combination with testosterone. Endocrinology 2003; 144:509–517.
35. Handelsman DJ, Spaliviero JA, Simpson JM, Allan CM, Singh J. Spermatogenesis without gonadotropins: maintenance has a lower testosterone threshold than initiation. Endocrinology 1999; 140: 3938–3946.
36. Pileri SA, Roncador G, Ceccarelli C, Piccioli M, Briskomatis A, Sabattini E, Ascani S, Santini D, Piccaluga PP, Leone O, Damiani S, Ercolessi C, et al. Antigen retrieval techniques in immunohistochemistry: comparison of different methods. J Pathol 1997; 183:116–123.
37. Allan CM, Couse JF, Simanainen U, Spaliviero J, Jimenez M, Rodriguez K, Korach KS, Handelsman DJ. Estradiol induction of spermatogenesis is mediated via an estrogen receptor-{alpha} mechanism involving neuroendocrine activation of follicle-stimulating hormone secretion. Endocrinology 2010; 151:2800–2810.
38. Pelletier RM. A novel perspective: the occluding zonule encircles the apex of the Sertoli cell as observed in birds. Am J Anat 1990; 188:87–108.
39. Setchell BP (ed.). Blood-testis barrier, junctional and transport proteins and spermatogenesis. In: Cheng CY, Austin TX (eds.), Molecular Mechanisms in Spermatogenesis. Landes Bioscience/Springer Science+-Business Media, LLC: New York; 2008:212–33.
40. Carette D, Weider K, Gilleron J, Giese S, Dompierre J, Bergmann M, Brehm R, Denizot JP, Segretain D, Pointis G. Major involvement of connexin 43 in seminiferous epithelial junction dynamics and male fertility. Dev Biol 2010; 346:54–67.
41. Lindsey JS, Wilkinson MF. Pem: a testosterone- and LH-regulated homeobox gene expressed in mouse Sertoli cells and epididymis. Dev Biol 1996; 179:471–484.
42. O'Shaughnessy PJ, Verhoeven G, De Gendt K, Monteiro A, Abel MH. Direct action through the sertoli cells is essential for androgen stimulation of spermatogenesis. Endocrinology 2010; 151:2343–2348.
43. Lim P, Robson M, Spaliviero J, McTavish KJ, Jimenez M, Zajac JD, Handelsman DJ, Allan CM. Sertoli cell androgen receptor DNA binding domain is essential for the completion of spermatogenesis. Endocrinology 2009; 150:4755–4765.
44. Abel MH, Baban D, Lee S, Charlton HM, O'Shaughnessy PJ. Effects of FSH on testicular mRNA transcript levels in the hypogonadal mouse. J Mol Endocrinol 2009; 42:291–303.
45. Nicholls PK, Harrison CA, Gilchrist RB, Farnworth PG, Stanton PG. Growth differentiation factor 9 is a germ cell regulator of Sertoli cell function. Endocrinology 2009; 150:2481–2490.
46. Li MW, Mruk DD, Lee WM, Cheng CY. Cytokines and junction restructuring events during spermatogenesis in the testis: an emerging concept of regulation. Cytokine Growth Factor Rev 2009; 20:329–338.
47. Yan HH, Mruk DD, Lee WM, Cheng CY. Blood-testis barrier dynamics are regulated by testosterone and cytokines via their differential effects on the kinetics of protein endocytosis and recycling in Sertoli cells. FASEB J 2008; 22:1945–1959.
48. Cameron DF, Muffly KE, Nazian SJ. Development of Sertoli cell binding competency in the peripubertal rat. J Androl 1998; 19:573–579.
49. Muffly KE, Nazian SJ, Cameron DF. Effects of follicle-stimulating hormone on the junction-related Sertoli cell cytoskeleton and daily sperm production in testosterone-treated hypophysectomized rats. Biol Reprod 1994; 51:158–166.
50. Sluka P, O'Donnell L, Bartles JR, Stanton PG. FSH regulates the formation of adherens junctions and ectoplasmic specialisations between rat Sertoli cells in vitro and in vivo. J Endocrinol 2006; 189:381–395.
51. Zhang FP, Pakarainen T, Poutanen M, Toppari J, Huhtaniemi I. The low gonadotropin-independent constitutive production of testicular testosterone is sufficient to maintain spermatogenesis. Proc Natl Acad Sci U S A 2003; 100:13692–13697.
52. Li MW, Mruk DD, Lee WM, Cheng CY. Connexin 43 and plakophilin-2 as a protein complex that regulates blood-testis barrier dynamics. Proc Natl Acad Sci U S A 2009; 106:10213–10218.
53. Domanskyi A, Zhang FP, Nurmio M, Palvimo JJ, Toppari J, Janne OA. Expression and localization of androgen receptor-interacting protein-4 in the testis. Am J Physiol Endocrinol Metab 2007; 292:E513–E522.